A multigenic program mediating breast cancer metastasis to bone

Yibin Kang,[1] Peter M. Siegel,[1] Weiping Shu,[1] Maria Drobnjak,[2] Sanna M. Kakonen,[3,4] Carlos Cordón-Cardo,[2] Theresa A. Guise,[3,5] and Joan Massagué[1,*]

[1]Cell Biology Program and Howard Hughes Medical Institute
[2]Department of Pathology
Memorial Sloan-Kettering Cancer Center, New York, New York
[3]Department of Molecular Medicine, University of Texas Health Science Center, San Antonio, Texas
[4]Present address: Schering Oy, PO Box 415, FIN-20101, Turku, Finland
[5]Present address: Division of Endocrinology and Metabolism, Department of Medicine, University of Virginia, Charlottesville, VA
*Correspondence: j-massague@ski.mskcc.org

Summary

We investigated the molecular basis for osteolytic bone metastasis by selecting human breast cancer cell line subpopulations with elevated metastatic activity and functionally validating genes that are overexpressed in these cells. These genes act cooperatively to cause osteolytic metastasis, and most of them encode secreted and cell surface proteins. Two of these genes, *interleukin-11* and *CTGF*, encode osteolytic and angiogenic factors whose expression is further increased by the prometastatic cytokine TGFβ. Overexpression of this bone metastasis gene set is superimposed on a poor-prognosis gene expression signature already present in the parental breast cancer population, suggesting that metastasis requires a set of functions beyond those underlying the emergence of the primary tumor.

Introduction

Metastasis, the spread and growth of tumor cells to distant organs, represents the most devastating attribute of cancer. A notable feature of this process is the variation in metastatic tissue tropism displayed by different types of cancer (Chambers et al., 2002; Fidler, 2002). In the case of breast cancer, most patients with advanced disease develop osteolytic bone metastases, which are a common cause of morbidity and sometimes mortality (Boyce et al., 1999; Mundy, 2002). An incomplete understanding of the molecular and cellular mechanisms underlying bone metastasis hinders the development of effective therapies that would eliminate or ameliorate this condition.

The establishment and growth of metastases at distant sites is thought to depend on interactions between tumor cells and the host environment. A classical view argues that during tumor progression, cancer cells acquire multiple alterations that render them increasingly competent to establish metastatic lesions in specific organs (Fidler and Kripke, 1977; Poste and Fidler, 1980). Many genes have been identified whose increased expression correlates with metastasis, and some have been shown to play a causal role in this process (Chambers et al., 2002; Woodhouse et al., 1997). How different genes may cooperate to fulfill various requirements for the establishment of tissue-specific metastases, and how the expression of metastasis-associated genes relates to the events that gave rise to the original tumor, remain important open questions. Indeed, primary tumors may already contain a gene expression profile that is strongly predictive of metastasis and poor survival, thus challenging the notion that metastatic ability is acquired late during tumor progression (Ramaswamy et al., 2003; van 't Veer et al., 2002).

We investigated these questions using the MDA-MB-231 human breast cancer cell line as a model system. These cells form typical osteolytic bone metastases when inoculated into the arterial circulation of mice. Their bone metastatic activity is enhanced by TGFβ (Yin et al., 1999), a ubiquitous cytokine that inhibits growth of normal epithelia and early stage tumors but stimulates invasion and metastasis of aggressive tumors (Derynck et al., 2001; Massagué et al., 2000). By in vivo selection of MDA-MB-231 cells, we have isolated subpopulations with enhanced metastatic abilities to either bone or the adrenal medulla. By comparing the transcriptomic profile of these isolates,

SIGNIFICANCE

Metastasis has long been thought to be the result of a small number of primary tumor cells acquiring certain genetic changes that allow them to spread to and thrive in distant organs. This concept was recently challenged by the proposal that metastasis may be directly driven by oncogenic mutations that exist in most cells of a primary tumor. Here we provide experimental evidence for the concept that breast cancer metastasis to a specific tissue—bone—is mediated by a specific set of genes. A small percentage of tumor cells in a human breast cancer cell line that possesses a recently described poor prognosis signature were able to metastasize to bone by virtue of overexpressing these genes. Our findings provide a conceptual framework and an experimental system for the identification of genes mediating metastasis to different organs.

we identified a gene set whose expression pattern is associated with, and promotes the formation of, metastasis to bone but not adrenal medulla. This gene expression profile is superimposed on a previously defined poor-prognosis gene expression signature (van 't Veer et al., 2002). Cells with the bone metastasis gene profile are present in the parental population and become selected in vivo as highly metastatic entities. Many genes in this group encode secretory or cell surface proteins implicated in cell homing to bone, angiogenesis, invasion, and osteoclast recruitment, thus influencing the tumor microenvironment in favor of metastasis. When overexpressed, these genes promote osteolytic bone metastasis by acting cooperatively. Two of these genes are further activated by TGFβ, suggesting a basis for the prometastatic activity of this cytokine in bone. The results point to key functions that must be acquired by poor-prognosis breast cancer cells in order to manifest their bone metastasis potential.

Results

In vivo selection of highly metastatic breast cancer cells

Cancer cell populations established from patients with advanced disease are thought to be heterogeneous, comprising different genomic characteristics and different abilities to metastasize to distant secondary sites. In vivo selection may prove effective in isolating highly metastatic subpopulations from the original mixture (Clark et al., 2000; Fidler, 1973). Therefore, we used this approach for the identification of circulating breast cancer cells with the ability to home and thrive at metastatic sites, especially bone (Figure 1A).

The breast cancer cell line MDA-MB-231 was isolated from the pleural effusion of a patient with disseminated disease relapsing several years after removal of the primary tumor (Cailleau et al., 1974). These cells form bone metastases from the bloodstream when inoculated into the left cardiac ventricle of immunodeficient mice (Yin et al., 1999). Bone metastases become detectable by X-ray imaging 10–12 weeks after inoculation of 10^5 parental MDA-MB-231 cells (obtained from the American Type Culture Collection, ATCC), and appear in 30% of inoculated animals (Figure 1B). Human tumor cells were recovered from such lesions, expanded in culture, and reinoculated into mice. Subpopulations 1833 and 2287 obtained after one cycle of in vivo selection generated large osteolytic bone lesions in only 5–7 weeks in most of the inoculated animals (Figures 1B and 1C; Table 1). Other populations obtained after one cycle of in vivo selection remained poorly metastatic to bone (Figures 1B and 1C), but some of them (e.g., 1834) exhibited high metastatic activity toward the adrenal medulla (data not shown).

Bone lesions generated by the 1833 and 2287 populations are very osteolytic, invading the bone matrix along the entire rim of the lesions they form (Figure 2A). These lesions incorporate numerous osteoclasts into the tumor mass and its periphery, as determined by TRAP (tartrate-resistant acid phosphatase) staining (Figure 2B). No TRAP-positive cells were observed in association with 1833 and 2287 cells when grown as subcutaneous tumors (data not shown). In contrast to the highly osteolytic nature of the bone lesions formed by 1833 and 2287, those eventually formed by 1834 and 1835, when allowed to grow to a similar size, had a smooth periphery pressing the bone matrix without invading it (Figure 2A), and recruited few TRAP-positive cells (Figure 2B). Of note, the 1833 and 2287 populations are not more aggressive than the parental population in the formation of subcutaneous tumors or proliferation in culture (data not shown). This suggests that the increased bone metastatic activity of these cells does not result from a faster growth rate, but rather from the acquisition of specific metastasis-promoting functions, including the ability to mobilize and recruit host osteoclasts.

Bone lesions generated by injection of 1833 were in turn expanded in vitro in order to isolate second-cycle metastatic populations. These secondary isolates were then tested for metastatic activity in vivo (Figure 1B), which demonstrated that the elevated bone metastatic activity of 1833 is a trait retained during passage in vitro or in vivo. A similar conclusion could be drawn for the 2287 cell population (data not shown). In comparison, second passage populations isolated from adrenal gland metastases by 1834 remained poorly metastatic to bone (Figure 1B) and highly metastatic to the adrenal gland (data not shown).

No enhanced expression of poor-prognosis gene expression signature in metastatic cells

A 70-gene expression signature strongly predictive of metastasis and poor survival was recently delineated by analysis of tumors from breast cancer patients (van 't Veer et al., 2002). We investigated the possibility that the enhanced metastatic abilities of the in vivo selected population might correlate with a gain in the expression of genes in this signature. Of 52 overexpressed genes in the poor-prognosis signature (van 't Veer et al., 2002), 38 are present in the Affymetrix U133A GeneChip. We compared the expression level of these genes in parental MDA-MB-231 cells and several highly metastatic derivative populations with the MCF10A, a cell line derived from normal human mammary epithelium as a control (Soule et al., 1990). Fourteen of the 38 genes are overexpressed in parental MDA-MB-231 compared to MCF10A, two are underexpressed, and the rest show little change (Figure 3A). This distribution is typical of breast tumors with poor outcome (van 't Veer et al., 2002). Of the 18 underexpressed genes in the poor-prognosis signature, ten are present in the U133A GeneChip. Seven of these were expressed at similar levels and three were overexpressed in parental MDA-MB-231 compared to MCF10A (Figure 3A). Overexpression of these three particular genes has been observed in several poor prognosis tumors (van 't Veer et al., 2002). Overall, then, the parental MDA-MB-231 population displays a previously defined poor-prognosis gene expression signature (van 't Veer et al., 2002). This is in agreement with the poor outcome of the particular case from which the MDA-MB-231 cell line was derived (Cailleau et al., 1974).

The expression pattern of the breast cancer prognosis genes in the highly metastatic subpopulations, however, showed little difference with that in the parental MDA-MB-231 population (Figure 3A). Thus, the gain in bone metastatic activity by MDA-MB-231 subpopulations does not involve an increased expression of these poor-prognosis signature genes.

Gene expression signature associated with osteolytic bone metastatic ability

We compared the transcriptional profile of parental MDA-MB-231 cells and twelve derivative subpopulations with different metastatic potentials in order to identify genes that differ in their expression between the weakly and the highly bone-metastatic

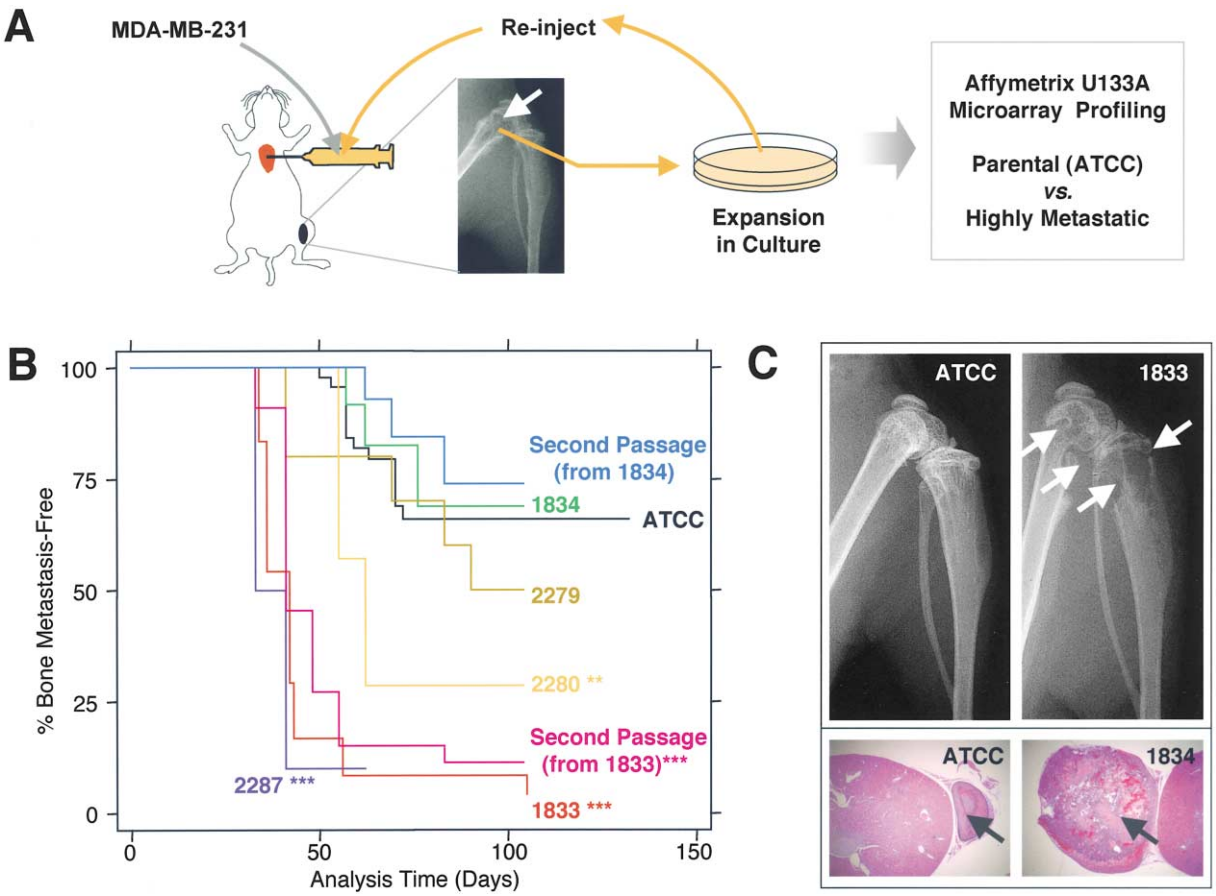

Figure 1. In vivo selection of highly metastatic breast cancer cells

A: Schematic representation of the in vivo selection process. MDA-MB-231 cells were inoculated into the left cardiac ventricle of nude mice. Bone lesions were detected by X-ray analysis 10–12 weeks after injection. Tumor cells were isolated from bone lesions and reinoculated after expansion in culture. Cells isolated from the second round of metastases were expanded in culture and reinoculated to confirm their metastatic phenotype. RNA samples isolated from these in vivo selected populations were subjected to gene expression profiling analysis to identify candidate metastasis-enhancing genes.

B: Kaplan-Meier curves showing the bone metastasis activity of the parental (ATCC) MDA-MB-231 cell population, various in vivo selected subpopulations, and various populations derived from a second in vivo passage of the latter, as listed in Table 1. Metastasis was scored as the time to first appearance of a visible bone lesion by X-ray imaging of the whole mouse. The percent of animals in each group that were free of detectable bone metastases is plotted. ** $p < 0.01$, *** $p < 0.001$ compared with the parental (ATCC). Data for second passage populations were pooled for the graphic representation; the data corresponding to each individual population are shown in Table 1.

C: Top: Representative X-ray radiography of the hindlimbs of mice six weeks after inoculation with the parental MDA-MB-231 (ATCC) or the 1833 highly metastatic population. Osteolytic lesions are indicated by arrows. Bottom: Representative H&E staining sections of the adrenal gland (arrows) from mice 12 weeks after inoculation of mice with parental MDA-MB-231 or the 1834 subpopulation. Large, bilateral adrenal metastases were evident in 1834 cell line, but not the parental cell line.

groups (Figure 3B). One hundred and two genes represented by 127 probe sets (Figure 3B) passed our filtering and statistical comparison criteria (see Experimental Procedures). Forty-three genes (52 probe sets) were selectively overexpressed in the highly metastatic set, and 59 (75 probe sets) were underexpressed (Figure 3B). Thus, the populations that are highly metastatic to bone have a distinct transcriptional signature not shared by populations that are highly metastatic to the adrenal gland. The identities of these genes are listed in the Supplemental Data at http://www.cancercell.org/cgi/content/full/3/6/537/DC1. Interestingly, none of the genes in the bone metastasis signature identified here are part of the previously defined poor-prognosis breast cancer signature (van 't Veer et al., 2002). Thus, the bone metastasis gene-expression profile identified here is nonoverlapping with, and superimposed on, a poor-prognosis gene expression signature present in the parental MDA-MB-231 cell population.

Most of the genes in this group that are overexpressed by more than 4-fold encode cell membrane or secretory products that may affect the host environment to favor metastasis (Figure 3C). They include the bone-homing chemokine receptor *CXCR4* (Muller et al., 2001; Taichman et al., 2002); the angiogenesis factors *fibroblast growth factor-5* (Giordano et al., 1996) and *connective tissue-derived growth factor* (Moussad and Brigstock, 2000); the activator of osteoclast differentiation *interleukin-11* (*IL11*, Manolagas, 1995); the matrix metalloproteinase/collagenase *MMP1*, which promotes osteolysis by cleaving a specific peptide bond in the collagen of bone matrix (Egeblad and Werb, 2002; Holliday et al., 1997; Zhao et al., 1999); *follistatin*, which binds activin blocking its growth inhibitory effects

Table 1. Incidence of bone metastasis generated by parental and various sublines of MDA-MB-231

MDA-MB-231 subline	Derived from	Site of isolation	Mice with bone met (%)	
			60 days	100 days
ATCC			8/45 (18%)	14/45 (31%)
1833	ATCC	Bone	22/25 (88%)	23/25 (92%)
1834	ATCC	Bone	1/15 (7%)	2/15 (13%)
2279	ATCC	Bone	2/10 (20%)	5/10 (50%)
2280	ATCC	Bone	3/9 (33%)	5/9 (56%)
2287	ATCC	Bone	9/10 (90%)	9/10 (90%)
2268	1833	Bone	5/5 (100%)	5/5 (100%)
2269	1833	Bone	9/9 (100%)	9/9 (100%)
2271	1833	Bone	5/9 (56%)	6/9 (67%)
2274	1833	Bone	9/10 (90%)	9/10 (90%)
2293	1834	Adrenal	0/5 (0%)	1/5 (20%)
2295	1834	Adrenal	0/5 (0%)	2/5 (40%)
2297	1834	Adrenal	0/5 (0%)	0/5% (0%)

The ratio of mice displaying bone metastases to the total number of mice is indicated for two time points, along with the percentage of mice bearing bone metastases (in parentheses). The origin of each cell population and the tissue from which it was isolated are also indicated.

(de Winter et al., 1996); the metalloproteinase-disintegrin family member *ADAMTS1* (Kuno et al., 1999); and *proteoglycan-1* (Timar et al., 2002).

The genes that are underexpressed in populations highly metastatic to bone form a functionally heterogeneous group including extracellular matrix components and receptors (*laminin β1*, *fibronectin*, *collagen type V*, *integrin β4*), cytoskeletal components (*tubulin α1*, *keratin 7*, *periplakin*), proteinases (*serpin A1*, *cathepsin B*), class II major histocompatibility complex components (*HLA-DPA1*, *-DPB1*, *-DPB3*), and putative tumor suppressors (*N33*, *DLC1*).

A functionally diverse set of genes cooperatively promote bone metastasis

Four of the most highly overexpressed genes in bone metastatic populations, *IL11*, *CTGF*, *CXCR4*, and *MMP-1*, each representing a distinct type of biological activity, were chosen to investigate their ability to promote bone metastasis in vivo. Northern blot analysis of all four gene transcripts (Figure 3D) confirmed the elevated expression of these genes in the populations highly metastatic to bone.

IL11 is a potent inducer of osteoclast formation from progenitor cells in the bone marrow (Manolagas, 1995). Osteoclasts are direct mediators of bone resorption in osteolytic bone metastases (Boyce et al., 1999; Mundy, 2002). We generated pools of *IL11*-transfected parental MDA-MB-231 cells (Figure 4A) and tested their metastatic activity in vivo. When overexpresed alone, IL11 did not significantly enhance bone metastasis formation by the parental population (Figure 4B). To search for genes that might collaborate with *IL11* in bone metastasis, we scrutinized microarray data for candidates. *Osteopontin (OPN)* is con-

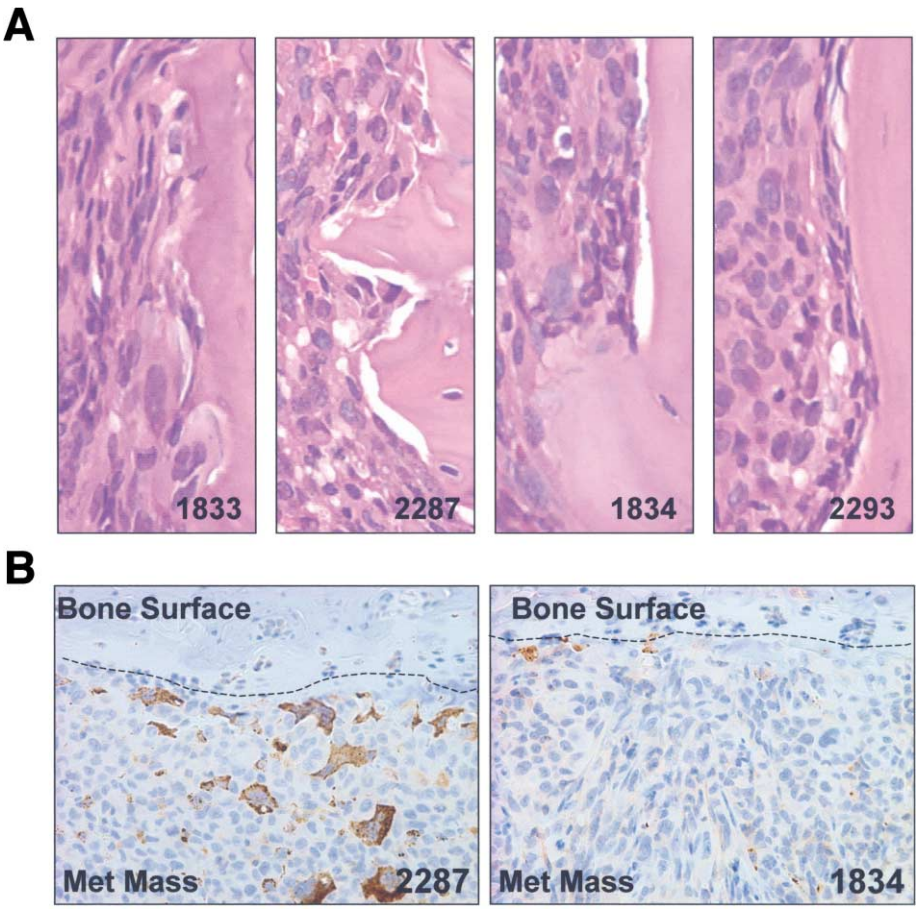

Figure 2. Osteoclast recruitment by highly osteolytic tumor cell populations

A: H&E staining of bone lesions generated by various in vivo selected populations with different metastatic potential to bone. In order to compare lesions of similar size, the lesions produced by the highly metastatic populations 6 weeks after inoculation were compared with lesions produced by the poorly metastatic populations 12 weeks after inoculation. The invasive nature of the highly metastatic populations 1833 and 2287 was evident in the rugged interface between tumor mass and the bone matrix. In comparison, this feature is rarely seen in lesions generated by the 1834 and 2293 populations. Instead, lesions generated by these two cell lines were mostly smooth and pressing against the bone matrix without invading it.

B: TRAP staining showing numerous osteoclasts in the tumor mass and tumor/bone interface in lesions generated by inoculation 2287 but not by 1834. Dotted line marks the bone matrix surface.

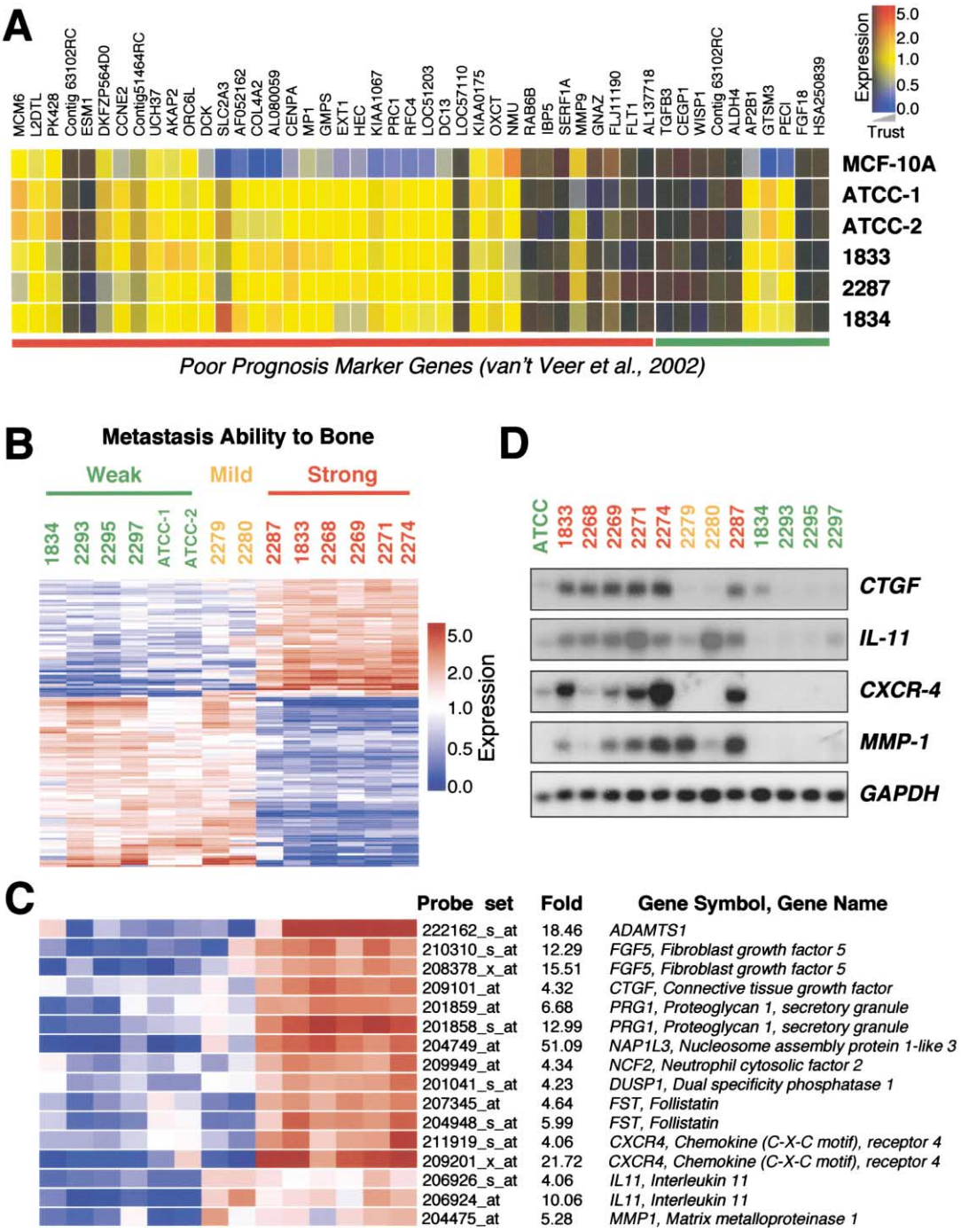

Figure 3. A bone metastasis gene expression signature

A: Expression pattern of a previously identified poor-prognosis breast cancer genes (van 't Veer et al., 2002) in the MCF-10A normal human mammary epithelial cell line, parental MDA-MB-231 cells, and three MDA-MB-231 subpopulations of different metastatic potential. Data correspond to the 48 out of the 70 poor-prognosis genes (van 't Veer et al., 2002) that are represented in the U133A GeneChip. Each column represents one gene, and each row one cell line. Genes that were expressed in higher or lower levels in poor prognosis tumors (van 't Veer et al., 2002) are underlined by red or green bars, respectively. Genes that were not expressed or expressed in very low level in all cell lines are shown in dark colors (low confidence).

B: Hierarchical cluster diagram of 127 filtered probe sets. Various in vivo selected cell lines were grouped according to their bone metastasis potential: weak (green), mild (yellow), and strong (red). ATCC-1 and ATCC-2 are duplicated samples of the parental MDA-MB-231 population. Criteria used to filter genes whose expression differs significantly between weak and strong metastatic groups are described in the Experimental Procedures. Each row represents one gene, and each column one cell line. Varying levels of expression are represented on a scale from dark blue (lowest expression) to dark red (highest expression).

C: Hierarchical cluster diagram of 11 genes (represented by 16 probe sets) among the 127 probe sets in **B** that differed by >4-fold in expression level between weak and strong metastatic groups. The Affymetrix probe set number, fold difference, and identities of the genes are indicated. ADAMTS-1: A disintegrin and metalloproteinase with thrombospondin motifs-1.

D: Confirmation of expression pattern of various metastasis-associated genes by Northern blot in the indicated cell populations.

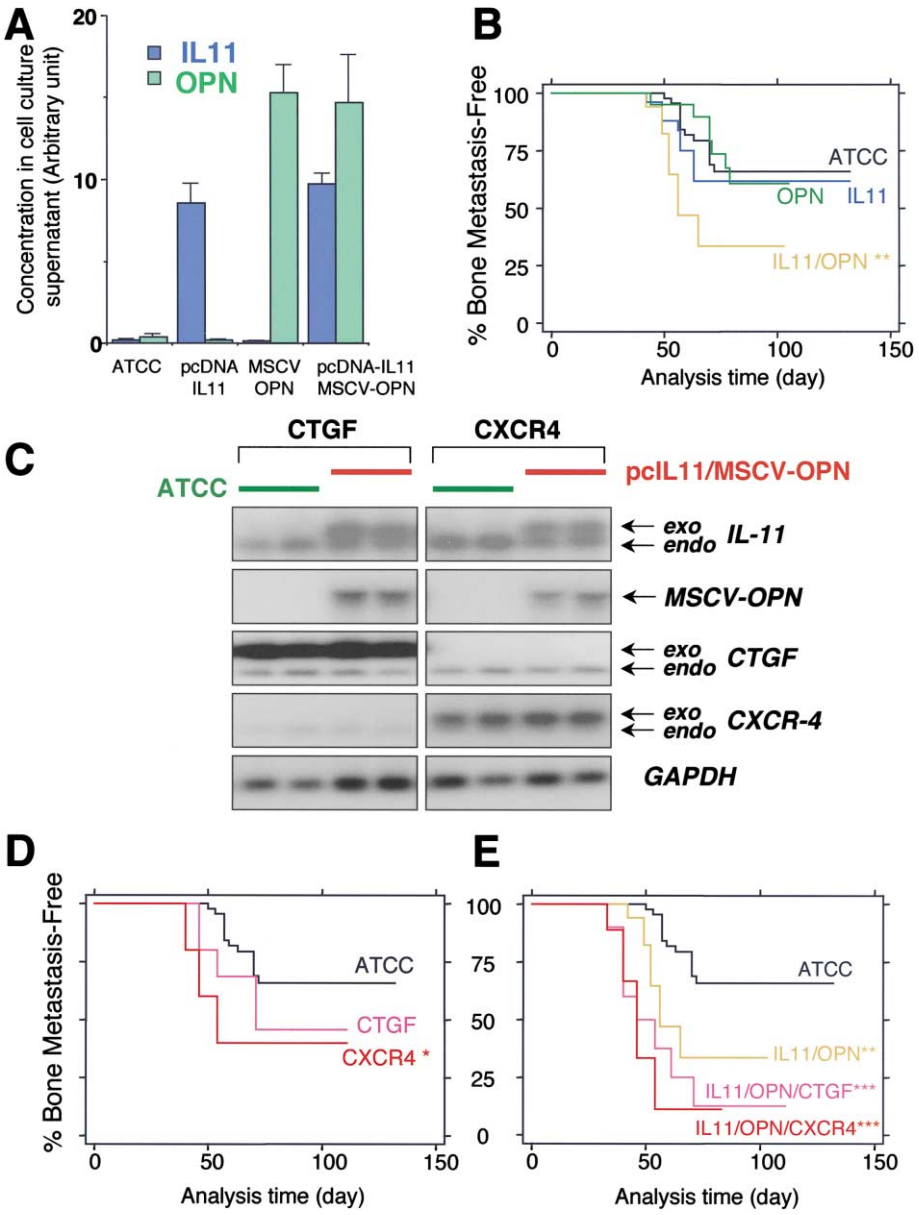

Figure 4. Cooperative metastatic activity of multiple bone metastasis genes

A: MDA-MB-231 cells were engineered to overexpress *IL11* or *osteopontin* (*OPN*) individually or together. Cell culture supernatants from each cell line were subjected to ELISA analysis for IL11 and OPN.

B, D, and E: Kaplan-Meier curves showing the incidence of bone metastasis by parental MDA-MB-231 cells (ATCC) and the indicated transfectant derivatives. * $p < 0.05$, ** $p < 0.01$, and *** $p < 0.001$ compared with the parental (ATCC).

C: Total RNA of different pools of single or triple transfectants used in **D** and **E** was harvested and subjected to Northern blot analysis using the indicated cDNA probes to confirm overexpression of exogenous genes. *Glyceraldehyde-3-phosphate dehydrogenase (GAPDH)* was used as a control.

sistently overexpressed in highly metastatic cells (Figure 6A, compare the first two lanes; and unpublished data), but was not present among the 102 filtered bone metastasis genes because it is also overexpressed in the cell populations that are highly metastatic to adrenal medulla (unpublished data). OPN is a secretory protein with multiple functions, including the ability to stimulate osteoclast adhesion to bone matrix (Asou et al., 2001; Denhardt et al., 2001). OPN has been implicated in cancer metastasis to various organs (Furger et al., 2001; Hotte et al., 2002; Reinholz et al., 2002; Weber, 2001). As IL11 and OPN play distinct roles in enhancing osteoclast function, we tested whether they could collaborate in promoting osteolytic bone metastasis. Indeed, the combined overexpression of *IL11* and *OPN* in parental MDA-MB-231 (Figure 4A) cells significantly augmented the incidence of bone metastasis (Figure 4B). Immunohistochemical analysis of the resulting lesions revealed the presence of numerous TRAP-positive cells (data not shown).

When overexpressed alone in parental MDA-MB-231 cells, *CXCR4* caused a limited but significant increase in bone metastasis formation, whereas *CTGF* did not (Figure 4D). However, triple transfectants overexpressing *IL11*, *OPN*, and either *CXCR4* or *CTGF* (Figure 4C) showed a dramatic increase both in the rate and in the incidence of bone metastases (Figure 4E). The aggressiveness of these triple transfectants approached that of the in vivo-selected highly metastatic populations. Preliminary data suggest that overexpression of *MMP1* alone or in combination with *IL11* and *OPN* also enhances bone metastasis. When grown as subcutaneous tumors or in culture, all these transfectants grew at the same rate as the parental cell population (data not shown). Thus, the combined activities of these genes specifically promote the growth of osteolytic bone metastases.

TGFβ activates bone metastasis genes *IL11* and *CTGF*

In normal epithelia and low-grade tumors, TGFβ acts as a potent growth inhibitor by causing cell cycle arrest or apoptosis (Massagué et al., 2000; Roberts and Sporn, 1990). The TGFβ receptors and their substrates and transcriptional mediators, the Smad proteins (Smad2 and Smad4), are tumor suppressors that suffer inactivating mutations in cancer (Derynck et al., 2001; Massagué et al., 2000). In breast cancer, however, tumor cells often show a selective loss of growth-inhibitory TGFβ response without a concurrent loss of TGFβ receptor or Smad functions (Chen et al., 2001; Derynck et al., 2001). In these cells, TGFβ may instead stimulate tumor invasion and metastasis, turning from a tumor suppressor into a tumor progression factor (Derynck et al., 2001). In mouse model systems, administration of TGFβ neutralizing agents decreases breast cancer metastasis (Muraoka et al., 2002; Yang et al., 2002). As TGFβ is abundantly stored in bone matrix (Mundy, 2002; Roberts and Sporn, 1990), it has been proposed that TGFβ released during osteolysis supports a cycle of metastatic breast cancer stimulation (Mundy, 2002).

MDA-MB-231 cells provide a good example of these alterations, as they suffer a selective loss of TGFβ antiproliferative gene responses (Chen et al., 2001) and a gain of bone metastatic TGFβ responsiveness in vivo (Yin et al., 1999). Metastasis formation by MDA-MB-231 cells is partly dependent on the ability of these cells to respond to TGFβ, as demonstrated by overexpression of dominant-negative and constitutively activated TGFβ receptors in the cell line (Yin et al., 1999). An elevated secretion of the osteolytic factor parathyroid-related protein (PTHrP) has been noted in TGFβ-stimulated MDA-MB-231 cells (Yin et al., 1999). However, this effect occurs without an increase in *PTHrP* mRNA levels, and is not augmented in our highly metastatic cell populations (unpublished data).

Among the bone metastasis genes identified here, *IL11* and *CTGF* have been previously reported to respond to TGFβ (Grotendorst et al., 1996; Morinaga et al., 1997). We observed a clear activation of these genes in the various cell populations used in our study (Figures 5A and 5B). In populations highly metastatic to bone, TGFβ further increased the already high level of *IL11* and *CTGF* expression (Figures 5A and 5B). The high basal expression of these genes in the highly metastatic populations did not result from autocrine stimulation by TGFβ, as determined by using TGFβ-neutralizing antibodies (data not shown).

The TGFβ signaling pathway involves Smad2 and Smad3 as direct substrates of the TGFβ receptor and Smad4 as their partner in the formation of transcriptional complexes (Massagué, 1998). To determine whether the Smad pathway participates in TGFβ-mediated induction of *IL11* and *CTGF* in MDA-MB-231 cells, we mapped the TGFβ responsive regions in the corresponding gene promoters (unpublished data) and used this information to perform chromatin immunoprecipitation (ChIP) assays (Figure 5C). TGFβ addition rapidly induced the binding of Smad2/3 and Smad4 to the relevant regions of the *IL11* and *CTGF* promoters. Therefore, *IL11* and *CTGF* induction via the canonical TGFβ/Smad pathway in the metastatic cells may participate in a bone metastasis cycle driven by paracrine TGFβ.

Evidence for in vivo selection of preexisting metastatic cells

We wished to determine whether the highly metastatic cells isolated through in vivo selection preexist in the parental MDA-MB-231 population. To this end, we isolated forty-six individual cells from the parental population by dilution cloning, and allowed them to multiply in culture. The resulting single-cell derived progenies were analyzed for the expression of five metastasis genes: *IL11*, *MMP1*, *CTGF*, *CXCR4*, and *OPN*. Several populations were found to overexpress four or five of these genes (Figure 6A). When these cells were inoculated into athymic mice, they formed bone metastases more aggressively than the parental population (Figure 6B), at a rate that was comparable to that of the in vivo-selected 1833 and 2287 populations (refer to Figure 1B). Populations overexpressing three of these genes (Figure 6A) had an intermediate metastatic activity (Figure 6B), and populations overexpressing just one were not more aggressive than the parental population (Figure 6B). Interestingly, populations that do not express any of these metastasis-associated genes failed to form detectable metastases for at least 8 months after inoculation (Figure 6B, and data not shown).

The single-cell progenies could be segregated into two groups, depending on the expression pattern of the 102 genes that constitute the in vivo-selected bone metastasis signature (Figure 6C). Remarkably, this gene expression pattern closely cosegregated with the metastatic activity of the single cell progenies. Multidimensional scaling (MDS) analysis of the expression pattern of the 102 genes provided further evidence for the relatedness of populations selected in vitro on the basis of expressing the five metastasis genes and populations selected in vivo on the basis of their high metastatic activity (Figure 6D). In the MDS analysis, these two sets of populations were clustered together, well separated from the poorly metastatic populations.

To compare the composition of the parental and the in vivo-selected highly metastatic populations, we isolated single-cell progenies from 1833 and 2287 cell lines. We then analyzed the expression pattern of bone metastasis genes in these single-cell progenies (Figure 6E). The proportion of cells expressing each of the metastasis genes tested was dramatically increased in the 1833 and 2287 cell lines compared to the parental population (Figure 6F).

We performed comparative genomic hybridization (CGH) analysis on the parental MDA-MB-231 population and its in vivo or in vitro selected derivatives with different metastatic potentials. As expected, the chromosomal profile of these different populations is highly aberrant compared to normal human cells (see Supplemental Data at http://www.cancercell.org/cgi/content/full/3/6/537/DC1). However, the profile of the different MDA-MB-231 subpopulations is very similar despite the marked differences in metastasis gene patterns and metastatic activities of these subpopulations. Some differences are present between the CGH profiles of the highly metastatic populations versus the weakly metastatic ones, including loss of chromosomal regions in 2q and 7q and gain in 12q and 14q. However, these differences are highly consistent among cells selected in vivo by their metastatic abilities or in vitro by their metastasis gene profile. Collectively, these results indicate that the bone metastasis gene expression pattern of populations 1833 and 2287 is not a result ongoing chromosomal alteration during the selection of these cells in vivo or their passage in vitro. We conclude that that the tumor-derived MDA-MB-231 population contains natural variants with a bone-metastasis gene signature and high metastatic activity to bone; these variants become selected in vivo by virtue of their high propensity to form fast-growing bone metastases.

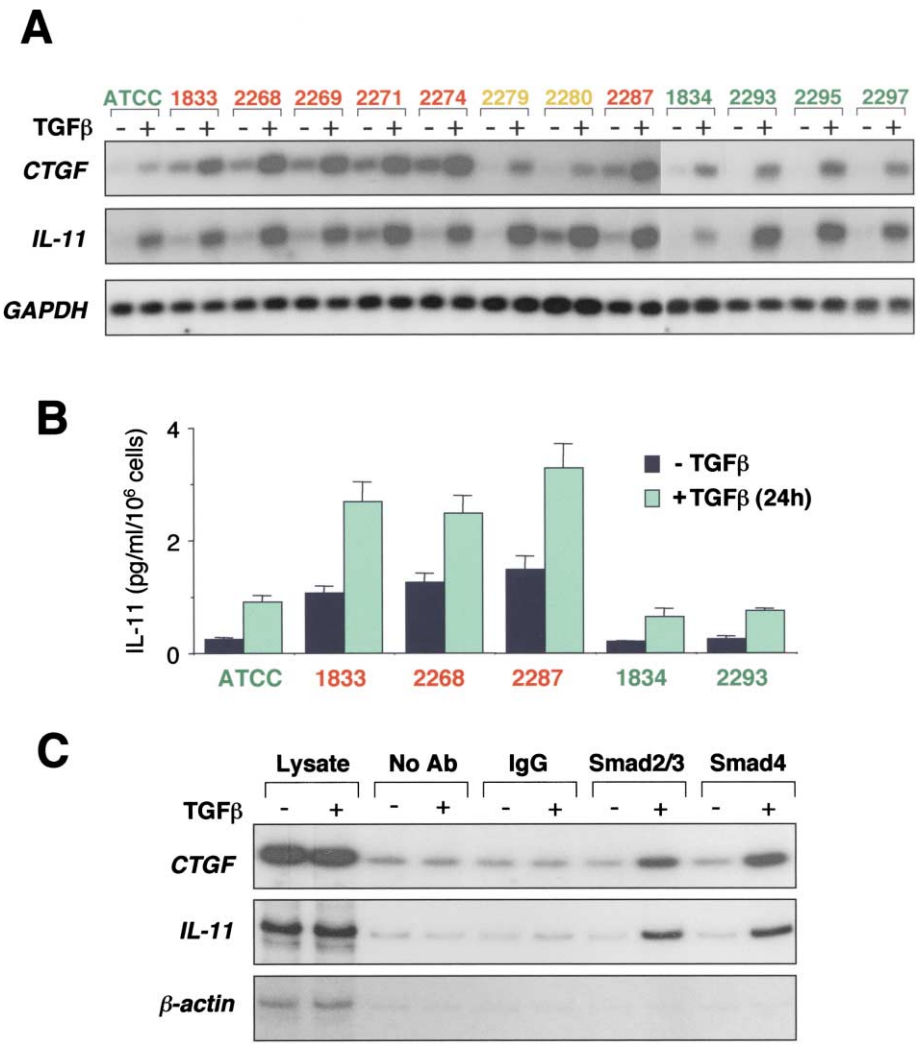

Figure 5. *IL11* and *CTGF* are transcriptional targets of TGFβ via the Smad pathway

A: Parental and derivative MDA-MB-231 populations were incubated in the presence (+) or absence (−) of 100 pM of TGFβ1 for 3 hr. Total RNA was subjected to Northern blot analysis with the indicated probes.

B: Cell cultures were washed and treated with TGFβ or no additions for 24 hr. IL11 production in the media was determined using an ELISA assay. Data are the average of triplicate determinations ± S.D.

C: MDA-MB-231 cells were left untreated (−) or treated (+) with TGFβ for 2 hr, and chromatin immunoprecipitations were performed with the indicated antibodies. PCR was performed with primers specific for the *IL11* and *CTGF* promoter regions encompassing the TGFβ responsive elements. Primers specific for the β-*actin* promoter were used for the negative controls.

Discussion

Only a fraction of the cells in the particular breast cancer population studied here have the ability to form highly aggressive, osteolytic bone metastases. A different fraction in the same population has the ability to form aggressive metastases in the adrenal medulla. Thus, metastatic ability is not a uniform trait in a breast cancer cell population.

The ability to form aggressive bone metastases is tightly associated with a distinctive expression profile of a defined set of genes. Cell populations isolated in vivo for their propensity to form bone metastases display this gene expression signature. Concordantly, single cell progenies that show this signature manifest a high propensity to form bone metastases. This signature is retained through repeated passage of the metastatic cell population in vitro and in vivo. Therefore, breast cancer cells with a defined tissue-specific metastatic ability preexist in the parental tumor cell population and have a distinctive bone metastasis gene expression signature. Formation of bone metastases is the result of selection and enrichment of these preexisting high expressers of the bone metastasis profile. Cell populations that are highly metastatic to the adrenal medulla do not share this gene expression signature, suggesting a basis for the tissue specificity.

The most prominently overexpressed genes in this bone metastasis signature encode mostly cell surface and secretory proteins, each of them with functions that may alter the host tissue environment to foster formation of osteolytic bone lesions (Figure 7). These functions (and the genes encoding them) include bone marrow homing and extravasation (*CXCR4*) (Muller et al., 2001), pericellular proteolysis and invasion (*MMP1*, *ADAMTS1*) (Egeblad and Werb, 2002; Holliday et al., 1997; Kuno et al., 1999), angiogenesis (*FGF5* and *CTGF*) (Giordano et al., 1996; Moussad and Brigstock, 2000), osteoclastogenesis (*IL11*) (Manolagas, 1995), growth factor regulation (*follistatin*) (de Winter et al., 1996), and extracellular matrix alteration (*proteoglycan-1*) (Timar et al., 2002).

Our functional assays provide evidence for a causal role of *IL11*, *CTGF*, and *CXCR4*, along with *OPN*, in osteolytic metastasis formation. High expression of *CXCR4* (Geminder et al., 2001; Muller et al., 2001; Taichman et al., 2002), *IL11* (Sotiriou et al., 2001), and *osteopontin* (Hotte et al., 2002; Reinholz et al., 2002) in human cancer has been clinically correlated with bone metastasis. For these particular genes, our work provides an important

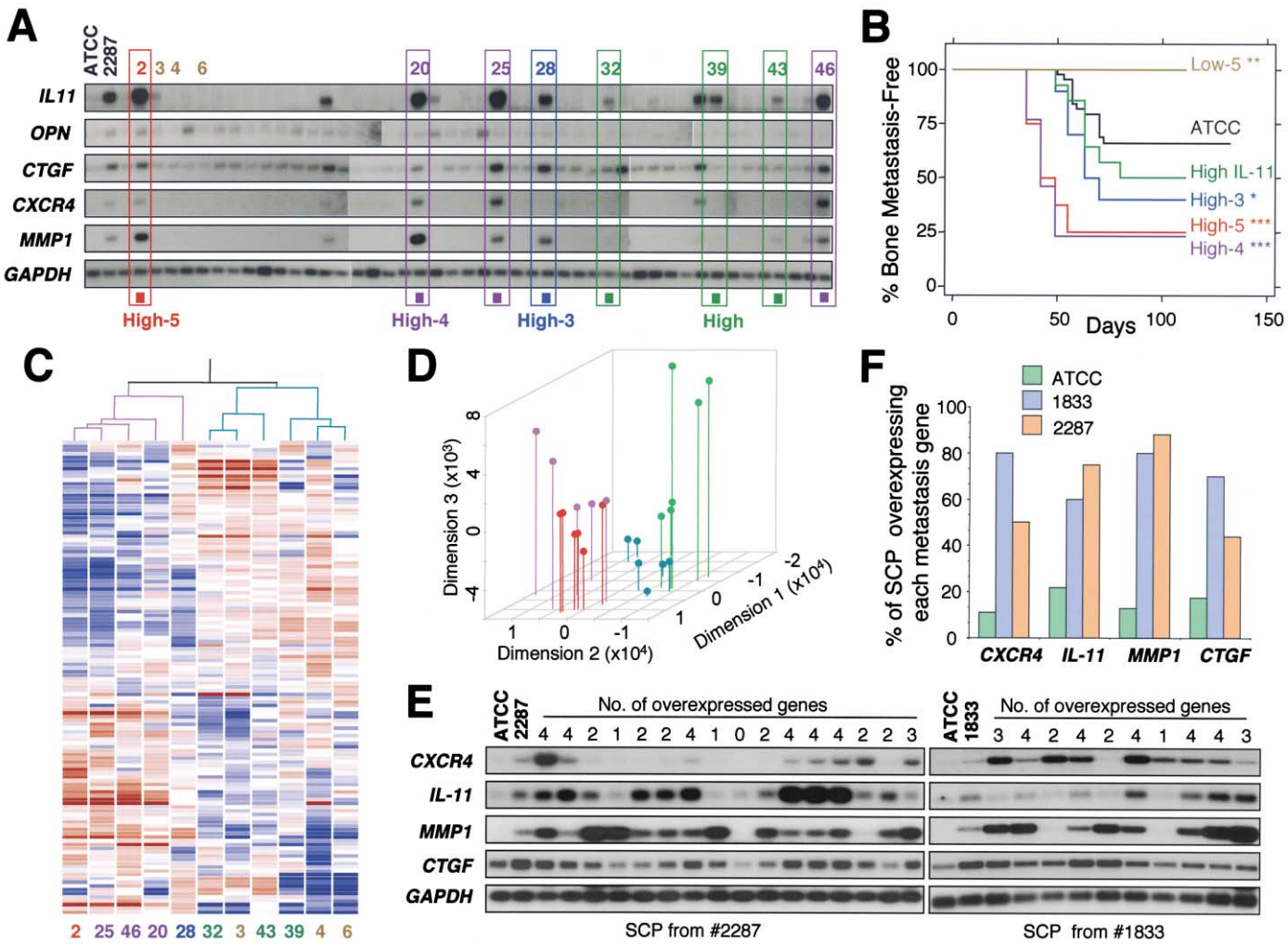

Figure 6. Evidence of in vivo selection of preexisting, highly metastatic cells

A: Forty-six single cells were randomly picked from the parental MDA-MB-231 population, expanded in culture, and subjected to Northern blot analysis using the six indicated probes. Cells tested in functional metastasis analysis are highlighted by colored boxes.

B: Kaplan-Meier curves showing the bone metastasis activity of the parental MDA-MB-231 population (ATCC) and the indicated single-cell derived populations. * $p < 0.05$ and *** $p < 0.001$ compared with parental cells. Cell lines that do not express any of the 5 genes generated no bone metastasis for up to 6 months after inoculation. Data for the High IL11 and High-4 groups were pooled.

C: Two-way hierarchical cluster diagram of the expression pattern of 127 filtered probe sets in 11 single-cell derived populations. In the dendrogram, populations are segregated into two major clusters that coincide with highly metastatic (purple) and weakly metastatic (teal) phenotypes. Each row represents one gene, and each column one cell line.

D: Multidimensional scaling plot illustrating the relationship among parental population, populations selected in vivo based on metastatic activity, and single-cell derived populations identified in vitro based on the expression pattern of 5 bone metastasis genes. Red and purple dots represent samples from the highly metastatic in vivo selected populations (Figure 3B) and single-cell derived populations, respectively. Green and teal dots represent samples from weakly metastatic in vivo selected populations (Figure 3B) and single-cell derived populations, respectively.

E: Sixteen and ten single cell progenies (SCPs) were randomly generated from the 1833 and 2287 populations, respectively, and subjected to Northern blot analysis using the indicated probes. Number of metastasis genes overexpressed in each SCP is indicated above each lane of samples.

The percentage of cells in parental, 1833, and 2287 populations overexpressing the indicated metastasis genes is summarized in **F**.

confirmation of their relevance to metastasis by showing functional evidence of their prometastatic effect in a mouse model. At the same time, their identification as prometastatic genes in our studies provides a validation of our approach as an unbiased means of identifying genes of relevance to human cancer metastasis. Most genes in our set, however, have not been shown to play a causal role in metastasis and could become potential candidates for new diagnostic markers and therapeutic targets.

Most of the bone metastasis genes identified here did not affect metastatic activity when individually overexpressed in poorly metastatic cells. However, the combined overexpression of as few as three of these genes—*IL11* and *OPN* combined with either *CXCR4* or *CTGF*—endowed cells with a level of metastatic activity close to that of the highly aggressive cell populations endogenously expressing the entire bone metastasis gene set. Formation of aggressive bone lesions therefore requires the cooperation of several genes that fulfill complementary functions.

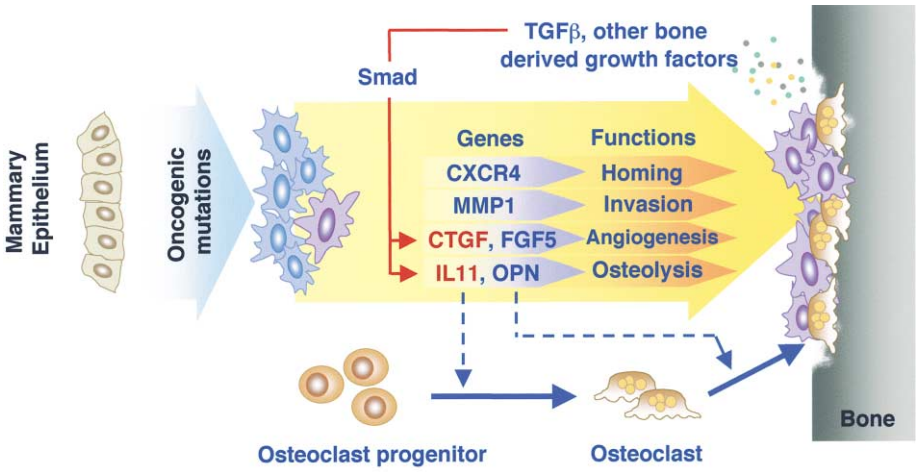

Figure 7. Bone-tropic metastasis is mediated by distinct classes of metastasis genes

A schematic model depicting molecular mechanisms underlying breast cancer metastasis as mediated by several of the genes in the present bone metastasis gene set. Primary breast tumor arises from normal mammary epithelium through the accumulation of oncogenic mutations. A small proportion of cancer cells in the primary tumor population accumulate additional genetic changes that mediate metastasis to the bone. Elevated expression of functionally distinct classes of metastasis-enhancing genes in these tumor cells cooperatively enables their invasion, colonization, and destruction of bone matrix. Destruction of bone matrix releases stored growth factors, including TGFβ, which causes a further increase in the expression of the TGFβ-responsive metastasis genes, *CTGF* and *IL11*, and establishes a positive feedback metastasis cycle.

The bone-specific metastasis genes identified here may additionally cooperate with genes that are not exclusive to the bone metastasis phenotype. Examples of the latter class include *PTHrP*, which is expressed in parental MDA-MB-231 cells and whose proosteolytic activity contributes to bone metastasis (Yin et al., 1999), and *OPN*, a multifunctional adhesion factor whose overexpression is observed in many metastatic tumors (Furger et al., 2001; Hotte et al., 2002; Reinholz et al., 2002; Weber, 2001). We observe *OPN* overexpression both in populations highly metastatic to bone and in those highly metastatic to adrenal medulla. In our functional assays, *OPN* promoted bone metastasis when overexpressed in combination with *IL11*. As an enhancer of osteoclast adhesion to bone matrix (Asou et al., 2001), OPN may leverage the osteoclast differentiation function of IL11 (Manolagas, 1995). Also relevant are the activities specifically decreased in the bone-metastatic populations, in particular several extracellular matrix proteins and proteases whose downregulation is in line with the important role of extracellular matrix alterations in invasion and metastasis (Cavallaro and Christofori, 2001; Hynes, 1976).

The long-standing hypothesis that metastatic cells are rare and arise late during tumor progression (Fidler and Kripke, 1977; Poste and Fidler, 1980) has been challenged by the finding that the clinical outcome of breast cancer patients can be predicted by a poor-prognosis gene expression signature present in the primary tumor (Bernards and Weinberg, 2002; Ramaswamy et al., 2003; van 't Veer et al., 2002). Our results may bridge the gap between these two views. In agreement with the latter hypothesis, we find that the parental MDA-MB-231 cell population possesses the poor-prognosis gene expression signature. However, we also find that additional functions, provided by a concrete set of bone metastasis genes, must be expressed in order to achieve an overt, tissue-specific metastasis phenotype. Thus, the bone metastasis gene expression signature identified here is superimposed on a poor-prognosis gene expression signature. We propose that the poor-prognosis gene expression signature enables the emergence of metastatic cells, whereas the bone metastasis gene expression signature identified here executes the metastatic potential of such cells.

The absence of an overlap between the present set of bone metastasis genes and a poor-prognosis gene expression signature may seem surprising. However, each of the genes that we have identified is likely to be utilized by only a fraction of breast cancer tumors metastasizing to bone, and their overexpression may emerge late in the course of the disease. On both counts, such genes would not score in studies seeking to identify bad prognosis signatures shared by a large proportion of primary tumor samples. The observed incidence of *CXCR4*, *IL11*, and *osteopontin* overexpression in clinical samples of metastatic tumors (Geminder et al., 2001; Hotte et al., 2002; Hynes, 1976; Muller et al., 2001; Sotiriou et al., 2001; Taichman et al., 2002) is consistent with these considerations.

Tumor progression is considered the result of cumulative oncogenic alterations. Once an original set of transforming events gives rise to a primary tumor, the tumor cells may accumulate further genetic and epigenetic alterations that dynamically affect their transcriptional profile. For cancer cells to metastasize to bone, certain complementary functions that may be irrelevant to primary tumor formation need to be progressively fulfilled. These functions include homing to the bone marrow, invasion, angiogenesis, or osteoclastogenesis. In the case of MDA-MB-231, these functions may be carried out by *CXCR4*, *CTGF*, *IL-11*, and *OPN*, with contributions from other genes in our gene set yet to be functionally tested. The functions contributed by *CXCR4*, *CTGF*, *IL-11*, or *OPN* could be fulfilled by different mediators in other tumors. The establishment of metastatic lesions may be driven by selection of a set of stochastically accumulated functions, rather than selection of a specific set of overexpressed genes. Therefore, a reiteration of the present experiments with other breast cancer cell models should provide a more complete view of alternative mediators of bone metastasis and a basis for the delineation of their incidence in the breast cancer patient population at large.

Experimental procedures

Intracardiac injections

Cell were harvested from subconfluent cell culture plates, washed with PBS, and resuspended at 10^6/ml concentrated in PBS. 0.1 ml of the suspended cells was injected into the left cardiac ventricle of 4-week-old, female BALB/c-nu/nu nude mice (NCI) using 26G needles as previously described (Yin et al., 1999). Mice were anesthetized with ketamine (100 mg/kg body weight) and xylazine (10 mg/kg body weight) before injection. A successful injection was characterized by the pumping of arterial blood into the syringe.

Radiographic analysis of bone metastasis

Development of bone metastases was monitored by X-ray radiography. Mice were anesthetized, arranged in prone position on single-wrapped films (X-OMAT AR, Eastman Kodak, Rochester, NY), and exposed to an X-ray at 35 kV for 15 s using a Faxitron instrument (Model MX-20; Faxitron Corp., Buffalo, IL, USA). Films were developed using a Konica SRX-101A processor and inspected for visible bone lesions.

Isolation of tumor cells from osteolytic bone lesions

To isolate tumor cells from the osteolytic lesions, mice with lesions detected by radiography were sacrificed, and the affected forelimbs or hindlimbs were separated from the body at the joints. Both ends of the long bone were cut open after skin and muscle were removed using a scalpel. A 1 ml syringe with a 26G needle was filled with PBS and inserted into one end of the bone. Mouse bone marrow cells as well as tumor cells were forced out from the other end by applying pressure to the syringe. Cells were collected by centrifuge and washed once with PBS before being cultured in 5 cm plates using regular MDA-MB-231 culture media. Mouse bone marrow cells did not attach to the plate and could be washed off with PBS after the tumor cells became attached. After one to two weeks of culture, a pure population of human cancer cells was obtained, as confirmed by FACS analysis using a FITC-conjugated anti-human HLA-A, B, C antibody (32294x, Pharmingen).

Histological analysis

Forelimb and hindlimb long bones of nude mice injected with cancer cells were excised, fixed in 10% neutral-buffered formalin, decalcified, and then embedded in paraffin and stained with hematoxylin and eosin (H&E). The kidneys and adrenal glands were removed from affected mice, fixed in 10% neutral-buffered formalin overnight, and dehydrated through a graded alcohol series and stored at 4 °C in 70% ethanol until processing. Following complete alcohol dehydration, the tissues were embedded in paraffin and H&E staining performed. Histological services were provided by Histoserv Inc. (Gaithersburg, MD).

For TRAP-staining, monoclonal mouse anti-TRAcP antibody (clone ZY-9C5; Zymed Laboratories, San Francisco, CA) was used at 1:50 final dilution. Avidin-biotin immunoperoxidase method with antigen retrieval was applied. Briefly, deparaffinized sections were treated with 1% H_20_2 to block endogenous peroxidase, followed by boiling sections in citric acid (0.01 M, pH 6.0) in a microwave oven for 15 min to enhance antigen retrieval. Mouse Ig blocking reagent (M.O.M Vector Laboratories, Inc, Burlingame, CA) and 10% normal horse serum were used to block nonspecific tissue reactivities. Primary antibody was applied for an overnight incubation at 4°C. Biotinylated horse anti-mouse IgG (Vector Laboratories, Inc) was used at 1:500 dilution for 30 min, followed by avidin-biotin complex (Vector Laboratories, Inc) at 1:25 dilution and 30 min incubation. Diaminobenzidine with 0.1% H_20_2 was used as the final chromogen and hematoxylin as the nuclear counterstain. Granular cytoplasmic staining was considered positive immunoreactivity.

Microarray data analysis

Absolute analysis of each chip was carried out using the Affymetrix Microarray Suite 5.0 Software to generate raw expression data. Parental and several in vivo selected sublines of MDA-MB-231 cell line were divided into two groups (weakly metastatic and highly metastatic, see Figure 2A) according to their metastatic potential to bone. To find genes that associated with metastasis phenotype, we applied three different filtering and statistical analysis constraints to the expression data to exclude those genes that did not vary significantly between comparison groups, or that were not expressed in a high enough level in either one of the two groups. First, statistical group comparison was carried out to find genes that show statistically significant differences in mean expression levels between the two groups. Log of ratio normalized expression data was analyzed with cross-gene error model turned on. Calculations without the assumption of equality of variances were done using Welch's approximate t test and ANOVA, with p value cutoff of 0.05. Benjamini and Hochberg false discovery rate was used for multiple testing correction. Of 22,283 genes in the Affymetrix U133A chip, 841 genes pass this restriction. Second, we applied expression level percentage restrictions, retaining only genes with minimum expression level over 1.5 in at least one of the two groups. 165 of 841 genes pass this restriction. Third, we used data quality flag restriction, retaining genes with flag value as Present (P) in at least 5 out of the total 12 samples. 102 of 165 genes pass this restriction. Of the 102 genes, 43 are overexpressed and 59 are underexpressed in the highly metastatic group. Detailed information about these 102 genes can be found in our Supplemental Data at http://www.cancercell.org/cgi/content/full/3/6/537/DC1.

We carried out one- or two-way hierarchical clustering analysis using the Genespring 5.0 software (Silicon Genetics). We used centroid linkage clustering with standard correlation as similarity metric. MDS was performed to visualize the similarity of gene expression profile between any pair of samples. Samples with similar gene expression profiles (shorter distances) were placed near each other in the three-dimensional MDS plot and separated from other dissimilar groups (longer distance). MDS analysis was carried out using an implementation in the R Statistical Software package downloaded from www.r-project.org. Data matrix and analysis commands could also be found in the Supplemental Data.

Single-cell derived populations

MDA-MB-231 cells were trypsinized, washed with PBS, and resuspended at 10 cells/ml, 5 cells/ml, and 2.5 cells/ml concentrations. 100 μl of each suspension was added to each well of a 96-well plate. After two weeks, wells harboring single colonies were identified by observation under microscope. Colonies were trypsinized from the well and expanded until reaching 80% confluency in a 10 cm tissue culture plate. Total RNA samples were harvested from each clone and subjected to Northern blot analyses.

ELISA analysis

The production and secretion of IL11 and OPN by parental MDA-MB-231 cells and various subpopulations or stable transfectants were determined in 24 hr-conditioned media using commercially available IL11 (R&D Systems) and OPN (Assay Designs, Inc.) ELISA kits according to the manufacturer's instructions.

Comparative genomic hybridization (CGH)

CGH was performed using standard procedures (Kallioniemi et al., 1992). Briefly, 1 μg DNA was labeled by nick translation using FITC-dUTP (NEN-DuPont) (cell line) or Texas Red-dUTP (NEN-DuPont) (normal female control), purified through spin columns, coprecipitated with 25 μg Cot-1 DNA (Invitrogen), resuspended in hybridization buffer, and hybridized to normal metaphase spreads for 48–72 hr. After standard stringency washes, the slides were stained with DAPI and mounted in Vectasheild mountant (Vector Labs). Image analysis was performed using the Isis digital imaging system (Metasystems). Data for CGH analysis can be found in the Supplemental Data.

Chromatin immunoprecipitation assay

ChIP assays were carried out as described (Takahashi et al., 2000) using MDA-MB-231 (ATCC) cells. Antibodies used were anti-Smad2/3 (Kretzschmar et al., 1999) and anti-Smad4 (Calonge and Massagué, 1999). Primer sets 5′-CCAACTTTTCCTTCCGTGCCC-3′ and 5′-GCATGTGCCCTGAGCA GCAGG-3′ were used to amplify a ~200 bp region of the *IL11* promoter containing the previously defined TGFβ responsive fragment. Primer sets 5′-CCTCTTCAGCTACCTACTTCC-3′ and 5′-GACATTCCTCGCATTCCTC CCCC-3′ were used to amplify a ~300 bp region of the *CTGF* promoter harboring a previously identified TGFβ responsive region. The primer set used to amplify the promoter region of β-*actin* was as described (Takahashi et al., 2000).

Statistical analysis

We created Kaplan-Meier survival curves using Stata 7.0 Software (Stata Corporation, College Station, TX). Log-rank test were used to calculate the statistical significance (p value) of difference between metastasis curves.

Acknowledgments

We are indebted to C.R. Chen, L. Jayaraman, J. Seoane, and D. Thomas for technical advice, A. Olshen for biostatistics support, and S. Tulley and E. Montalvo for expert technical assistance. We thank R. Benezra, L. Norton, N. Rosen, H. Varmus, A. Viale, and members of our laboratory for insightful discussion. We acknowledge the use of the Genomics Core Facility, Molecular Cytogenetics Core Facility, and the Flow Cytometry Core Facility at MSKCC, and in particular the expert technical support of H. Zhao in MDS

analysis and M. Leversha in CGH analysis. Y.K. and P.M.S. are the recipients of postdoctoral fellowships from the Irvington Institute for Immunological Research and the Damon Runyon-Walter Winchell Cancer Fund, respectively. J.M. is an Investigator of the Howard Hughes Medical Institute. This research is also supported by NIH grant P01-CA94060 (J.M.) and R01-CA69158 (T.A.G).

Received: February 10, 2003
Revised: May 14, 2003
Published: June 23, 2003

References

Asou, Y., Rittling, S.R., Yoshitake, H., Tsuji, K., Shinomiya, K., Nifuji, A., Denhardt, D.T., and Noda, M. (2001). Osteopontin facilitates angiogenesis, accumulation of osteoclasts, and resorption in ectopic bone. Endocrinology *142*, 1325–1332.

Bernards, R., and Weinberg, R.A. (2002). A progression puzzle. Nature *418*, 823.

Boyce, B.F., Yoneda, T., and Guise, T.A. (1999). Factors regulating the growth of metastatic cancer in bone. Endocr. Relat. Cancer *6*, 333–347.

Cailleau, R., Young, R., Olive, M., and Reeves, W.J., Jr. (1974). Breast tumor cell lines from pleural effusions. J. Natl. Cancer Inst. *53*, 661–674.

Calonge, M.J., and Massagué, J. (1999). Smad4/DPC4 silencing and hyperactive Ras jointly disrupt transforming growth factor β antiproliferative responses in colon cancer cells. J. Biol. Chem. *274*, 33637–33643.

Cavallaro, U., and Christofori, G. (2001). Cell adhesion in tumor invasion and metastasis: loss of the glue is not enough. Biochim. Biophys. Acta *1552*, 39–45.

Chambers, A.F., Groom, A.C., and MacDonald, I.C. (2002). Dissemination and growth of cancer cells in metastatic sites. Nat. Rev. Cancer *2*, 563–572.

Chen, C.R., Kang, Y., and Massagué, J. (2001). Defective repression of c-myc in breast cancer cells: A loss at the core of the transforming growth factor β growth arrest program. Proc. Natl. Acad. Sci. USA *98*, 992–999.

Clark, E.A., Golub, T.R., Lander, E.S., and Hynes, R.O. (2000). Genomic analysis of metastasis reveals an essential role for RhoC. Nature *406*, 532–535.

de Winter, J.P., ten Dijke, P., de Vries, C.J., van Achterberg, T.A., Sugino, H., de Waele, P., Huylebroeck, D., Verschueren, K., and van den Eijnden-van Raaij, A.J. (1996). Follistatins neutralize activin bioactivity by inhibition of activin binding to its type II receptors. Mol. Cell. Endocrinol. *116*, 105–114.

Denhardt, D.T., Giachelli, C.M., and Rittling, S.R. (2001). Role of osteopontin in cellular signaling and toxicant injury. Annu. Rev. Pharmacol. Toxicol. *41*, 723–749.

Derynck, R., Akhurst, R.J., and Balmain, A. (2001). TGF-β signaling in tumor suppression and cancer progression. Nat. Genet. *29*, 117–129.

Egeblad, M., and Werb, Z. (2002). New functions for the matrix metalloproteinases in cancer progression. Nat. Rev. Cancer *2*, 161–174.

Eischen, C.M., Weber, J.D., Roussel, M.F., Sherr, C.J., and Cleveland, J.L. (1999). Disruption of the ARF-Mdm2-p53 tumor suppressor pathway in Myc-induced lymphomagenesis. Genes Dev. *13*, 2658–2669.

Fidler, I.J. (1973). Selection of successive tumour lines for metastasis. Nat. New Biol. *242*, 148–149.

Fidler, I.J. (2002). Critical determinants of metastasis. Semin. Cancer Biol. *12*, 89–96.

Fidler, I.J., and Kripke, M.L. (1977). Metastasis results from preexisting variant cells within a malignant tumor. Science *197*, 893–895.

Furger, K.A., Menon, R.K., Tuckl, A.B., Bramwelll, V.H., and Chambers, A.F. (2001). The functional and clinical roles of osteopontin in cancer and metastasis. Curr. Mol. Med. *1*, 621–632.

Geminder, H., Sagi-Assif, O., Goldberg, L., Meshel, T., Rechavi, G., Witz, I.P., and Ben-Baruch, A. (2001). A possible role for CXCR4 and its ligand, the CXC chemokine stromal cell-derived factor-1, in the development of bone marrow metastases in neuroblastoma. J. Immunol. *167*, 4747–4757.

Giordano, F.J., Ping, P., McKirnan, M.D., Nozaki, S., DeMaria, A.N., Dillmann, W.H., Mathieu-Costello, O., and Hammond, H.K. (1996). Intracoronary gene transfer of fibroblast growth factor-5 increases blood flow and contractile function in an ischemic region of the heart. Nat. Med. *2*, 534–539.

Grotendorst, G.R., Okochi, H., and Hayashi, N. (1996). A novel transforming growth factor beta response element controls the expression of the connective tissue growth factor gene. Cell Growth Differ. *7*, 469–480.

Holliday, L.S., Welgus, H.G., Fliszar, C.J., Veith, G.M., Jeffrey, J.J., and Gluck, S.L. (1997). Initiation of osteoclast bone resorption by interstitial collagenase. J. Biol. Chem. *272*, 22053–22058.

Hotte, S.J., Winquist, E.W., Stitt, L., Wilson, S.M., and Chambers, A.F. (2002). Plasma osteopontin: associations with survival and metastasis to bone in men with hormone-refractory prostate carcinoma. Cancer *95*, 506–512.

Hynes, R.O. (1976). Cell surface proteins and malignant transformation. Biochim. Biophys. Acta *458*, 73–107.

Kallioniemi, A., Kallioniemi, O.P., Sudar, D., Rutovitz, D., Gray, J.W., Waldman, F., and Pinkel, D. (1992). Comparative genomic hybridization for molecular cytogenetic analysis of solid tumors. Science *258*, 818–821.

Kretzschmar, M., Doody, J., Timokhina, I., and Massagué, J. (1999). A mechanism of repression of TGFβ/Smad signaling by ongenic ras. Genes Dev. *13*, 804–816.

Kuno, K., Terashima, Y., and Matsushima, K. (1999). ADAMTS-1 is an active metalloproteinase associated with the extracellular matrix. J. Biol. Chem. *274*, 18821–18826.

Manolagas, S.C. (1995). Role of cytokines in bone resorption. Bone *17*, 63S–67S.

Massagué, J. (1998). TGFβ signal transduction. Annu. Rev. Biochem. *67*, 753–791.

Massagué, J., Blain, S.W., and Lo, R.S. (2000). TGFβ signaling in growth control, cancer, and heritable disorders. Cell *103*, 295–309.

Morinaga, Y., Fujita, N., Ohishi, K., and Tsuruo, T. (1997). Stimulation of interleukin-11 production from osteoblast-like cells by transforming growth factor β and tumor cell factors. Int. J. Cancer *71*, 422–428.

Moussad, E.E., and Brigstock, D.R. (2000). Connective tissue growth factor: what's in a name? Mol. Genet. Metab. *71*, 276–292.

Muller, A., Homey, B., Soto, H., Ge, N., Catron, D., Buchanan, M.E., McClanahan, T., Murphy, E., Yuan, W., Wagner, S.N., et al. (2001). Involvement of chemokine receptors in breast cancer metastasis. Nature *410*, 50–56.

Mundy, G.R. (2002). Metastasis to bone: causes, consequences and therapeutic opportunities. Nat. Rev. Cancer *2*, 584–593.

Muraoka, R.S., Dumont, N., Ritter, C.A., Dugger, T.C., Brantley, D.M., Chen, J., Easterly, E., Roebuck, L.R., Ryan, S., Gotwals, P.J., et al. (2002). Blockade of TGF-β inhibits mammary tumor cell viability, migration, and metastases. J. Clin. Invest. *109*, 1551–1559.

Poste, G., and Fidler, I.J. (1980). The pathogenesis of cancer metastasis. Nature *283*, 139–146.

Ramaswamy, S., Ross, K.N., Lander, E.S., and Golub, T.R. (2003). A molecular signature of metastasis in primary solid tumors. Nat. Genet. *33*, 49–54.

Reinholz, M.M., Iturria, S.J., Ingle, J.N., and Roche, P.C. (2002). Differential gene expression of TGF-β family members and osteopontin in breast tumor tissue: analysis by real-time quantitative PCR. Breast Cancer Res. Treat. *74*, 255–269.

Roberts, A.B., and Sporn, M.B. (1990). The transforming growth factor-betas. In Peptide Growth Factors and Their Receptors, M.B. Sporn and A.B. Roberts, eds. (Heidelberg: Springer-Verlag), pp. 419–472.

Sotiriou, C., Lacroix, M., Lespagnard, L., Larsimont, D., Paesmans, M., and

Body, J.J. (2001). Interleukins-6 and -11 expression in primary breast cancer and subsequent development of bone metastases. Cancer Lett. *169*, 87–95.

Soule, H.D., Maloney, T.M., Wolman, S.R., Peterson, W.D., Jr., Brenz, R., McGrath, C.M., Russo, J., Pauley, R.J., Jones, R.F., and Brooks, S.C. (1990). Isolation and characterization of a spontaneously immortalized human breast epithelial cell line, MCF-10. Cancer Res. *50*, 6075–6086.

Taichman, R.S., Cooper, C., Keller, E.T., Pienta, K.J., Taichman, N.S., and McCauley, L.K. (2002). Use of the stromal cell-derived factor-1/CXCR4 pathway in prostate cancer metastasis to bone. Cancer Res. *62*, 1832–1837.

Takahashi, Y., Rayman, J.B., and Dynlacht, B.D. (2000). Analysis of promoter binding by the E2F and pRB families in vivo: distinct E2F proteins mediate activation and repression. Genes Dev. *14*, 804–816.

Timar, J., Lapis, K., Dudas, J., Sebestyen, A., Kopper, L., and Kovalszky, I. (2002). Proteoglycans and tumor progression: Janus-faced molecules with contradictory functions in cancer. Semin. Cancer Biol. *12*, 173–186.

van 't Veer, L.J., Dai, H., van de Vijver, M.J., He, Y.D., Hart, A.A., Mao, M., Peterse, H.L., van der Kooy, K., Marton, M.J., Witteveen, A.T., et al. (2002). Gene expression profiling predicts clinical outcome of breast cancer. Nature *415*, 530–536.

Weber, G.F. (2001). The metastasis gene osteopontin: a candidate target for cancer therapy. Biochim. Biophys. Acta *1552*, 61–85.

Woodhouse, E.C., Chuaqui, R.F., and Liotta, L.A. (1997). General mechanisms of metastasis. Cancer *80*, 1529–1537.

Yang, Y.A., Dukhanina, O., Tang, B., Mamura, M., Letterio, J.J., MacGregor, J., Patel, S.C., Khozin, S., Liu, Z.Y., Green, J., et al. (2002). Lifetime exposure to a soluble TGF-β antagonist protects mice against metastasis without adverse side effects. J. Clin. Invest. *109*, 1607–1615.

Yin, J.J., Selander, K., Chirgwin, J.M., Dallas, M., Grubbs, B.G., Wieser, R., Massagué, J., Mundy, G.R., and Guise, T.A. (1999). TGF-β signaling blockade inhibits PTHrP secretion by breast cancer cells and bone metastases development. J. Clin. Invest. *103*, 197–206.

Zhao, W., Byrne, M.H., Boyce, B.F., and Krane, S.M. (1999). Bone resorption induced by parathyroid hormone is strikingly diminished in collagenase-resistant mutant mice. J. Clin. Invest. *103*, 517–524.